ISSN (Print) 1226-1750
ISSN (Online) 2233-6656
Journal of Magnetics 28(2), 219-226 (2023) https://doi.org/10.4283/JMAG.2023.28.2.219

Multislice Analysis of Axial Flux Synchronous Reluctance Motor Based on 2d Finite Element Method Linear Model

Emre Gözüaçık[1], Mustafa Eker[2]*, and Mehmet Akar[1]

[1]*Department of Electrical and Electronics Engineering, Tokat Gaziosmanpaşa University, 60150, Turkey*
[2]*Department of Electrical and Electronics Engineering, Institute of Graduate Studies, Tokat Gaziosmanpaşa University, 60150, Turkey*

(Received 9 February 2023, Received in final form 11 May 2023, Accepted 15 May 2023)

This study proposes a solution to improve the analysis time of the Axial Flux Synchronous Reluctance Motor (AF-SynRM) using the Finite Element Method (FEM) using the Finite Element Method (FEM). While accurate results can be achieved through 2D and 3D FEM analyses in the design of electrical machines, the analysis time becomes a significant consideration. The non-axisymmetric structure of the flux path in axial flux motors poses challenges for accurate results in 2D FEM analyses. To overcome this issue, the study uses simulation studies to convert axial flux motors into 2D linear models. In this study, a slice model approach is implemented in the linear structure, and the influence of the number of slices on various motor parameters, such as torque, torque ripple, back-EMF, loss, and efficiency, is analyzed and compared with 3D FEM analyses. Experimental loss and efficiency results are also included in these analyses. This study is the first to simulate an AF-SynRM in the 2D linear model. The accuracy of the results is verified experimentally.

Keywords : axial flux synchronous reluctance motor, multislice model, 2D linear model, FEM

1. Introduction

Synchronous reluctance motors are characterized by their simple structure, as the rotor core is made solely of ferromagnetic material. These motors offer high efficiency due to minimal rotor losses and cost-effectiveness attributed to the absence of magnets in their construction [1]. Axial flux machines have higher power and torque density than radial flux machines. In addition to its robust and compact structure also has less volume due to its shorter axial length [2, 3]. Notably, Axial Flux Synchronous Reluctance Motors (AF-SynRM) benefit from a shorter flux path, contributing to a higher power-to-weight ratio [4].

Radial machines can be analyzed using 2D Finite Element Method (FEM) due to their axisymmetric structure. However, axial machines have a non-axisymmetric design with a 3D flux path, thus requiring 3D FEM analysis for modeling [5]. Despite improved software for FEM analysis and reduced computational time, 3D FEM analysis remains time-consuming for designers. Due to the complex calculations and 3D problems, these analyses take longer time [6]. 2D FEM analyses have also been developed for axial flux machines to shorten this time and facilitate the design phase.

In a simple 2D model of AF-SynRM, a single slice 2D FEM model is constructed using averaged spatial parameters to make the machine an equivalent linear motor model. This model, known as the Linear Motor Modeling Approach, involves constructing a single slice 2D FEM model by averaging the spatial parameters of the machine, such as the inner and outer radii [7]. Other variations of linear models, such as the Inner Rotor Modeling Approach and Outer Rotor Modeling Approach, exist in the literature, where different inner and outer diameters are considered based on various radius cuts [5]. In the Quesi-3D model, the axial machine can be considered as consisting of several linear machines, and the performances of these machines are analyzed to represent the overall performance of the axial flux machine [8]. This approach allows for the consideration of variables related to the conical structure of the machine, such as the magnet structure, tooth width, and barrier structure.

In [5, 8-11], 2D linear and 3D model analyses are compared. The results have shown that the 2D model yields close results to the 3D model, while significantly

*Corresponding author: Tel: +90-3562521616-2967
e-mail: mustafa.eker@gop.edu.tr

reducing the analysis time. In [7], both single-slice and multi-slice 2D models were examined using up to 16 slices. The results showed that the 2D models produced results that were in good agreement with the 3D model analysis. In [12], it was suggested that a 2D model of a motor operating under load is a fast alternative for evaluating torque ripple, compared to using a 3D model.

This study tests 2D multislice model approaches using the multislice method of AF-SynRM for the first time. The comparison is made among the test results of a prototype AF-SynRM, the 3D analysis results, and the 2D analysis results obtained by varying the number of slices. The analyses were performed for both 3D FEM and 2D FEM using a constant current source and the current angle that gives the best values according to the MTPA method. The design study at [13] tested the accuracy of this type of excitation. Parametric analyses were also added to these analyses depending on the load variation. It is aimed to realize the 2D linear model analysis results with a minimum deviation compared to the 3D analysis results. In this way, the 2D FEM model is expected to provide reliable and efficient results in a shorter timeframe, thereby facilitating the work of the designer.

2. Finite Element Method Modeling

2.1. 3D Finite Element Method Modelling

The 3D FEM analysis allows the simulation of the machine by generating a mesh structure depending on the coordinates, machine parameters, connections, material types, and boundary conditions [14, 15]. The analysis time is influenced by factors such as the number of meshes, step density, and the variability of machine parameters. Fig. 1 shows the FEM analysis of the AF-SynRM 1/8 3D solid model.

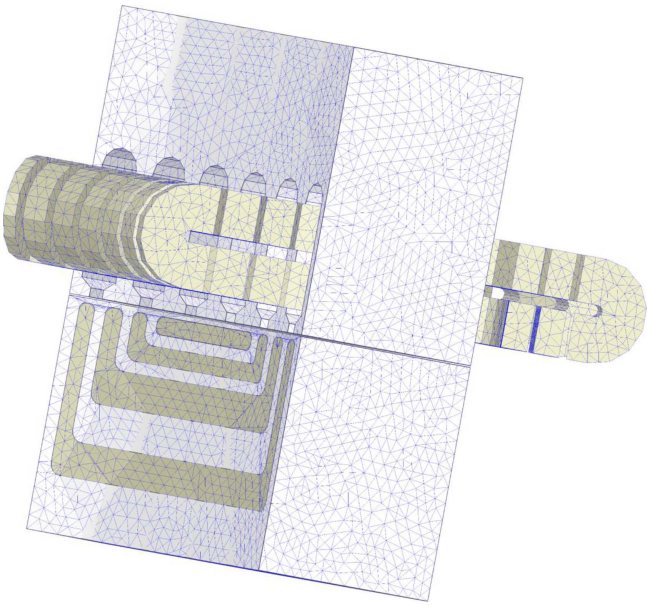

Fig. 1. (Color online) AF-SynRM Motor 3D Model Mesh Analysis.

Table 1. Main properties of AF-SynRM.

Parameters	Value
Output Power (W)	2200
Speed (rpm)	1500
Efficiency (%)	90
Power Factor	0.7
Air Gap (mm)	0.3
Pole Number	8
Outer Diameter (mm)	210
Inner Diameter (mm)	150

Axial flux machines are defined as 3D problems due to their 3D flux distributions compared to radial flux machines. The flux density distribution in the air gap varies depending on the angular change in the axis of rotation and the radial dimension. As a result, accurate calculations require a 3D modeling approach [9, 16]. The parameters used in the AF-SynRM design are given in Table 1 [13].

2.2. 2D Finite Element Method Modelling

The transformation of the 3D machine into an equivalent 2D linear model imposes some limitations for accurate motor performance prediction. Firstly, the radial direction is assumed to be an infinite length in the 2D model. This means that the final effect of the flux and the end winding reactance are neglected [17]. The 2D linear model transformation can be expressed as modeling the 2D domain cut by a virtual plane through the mean diameter of the outer and inner diameters of the axial flux machine. The linear approximation of the 3D model also allows for a multislice approach [6, 18]. The 2D linear model based on the mean diameter of the 3D model is given in Fig. 2.

The average diameter should be calculated for each slice of the machine divided into slices using the multislice method, and the design should proceed accordingly. The calculation of the average diameter (D_{avg}) is given in Eq. (1) [8].

$$D_{avg,i} = D_{out} - j.\frac{L_s}{N} \tag{1}$$

$$L_s = \frac{D_{out} - D_{in}}{2} \tag{2}$$

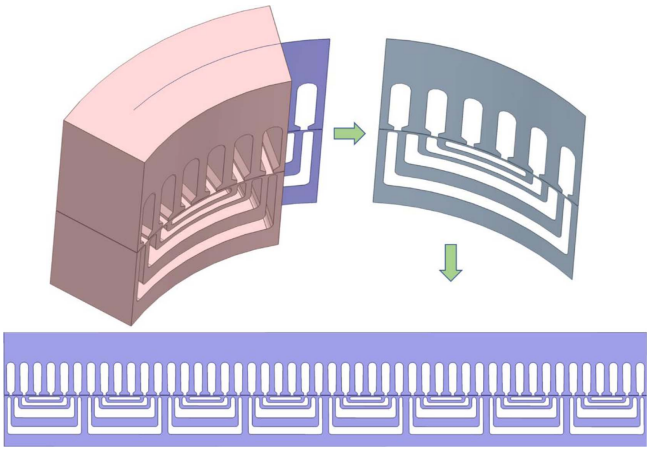

Fig. 2. (Color online) AF-SynRM 1/8 3D Solid Model and Simulation of 2D Linear Model.

$$j = 2i - 1, \qquad i = 1, 2, 3..., N \tag{3}$$

$$L = \pi . D_{avg} \tag{4}$$

The outer diameter D_{out}, the inner diameter D_{in}, slice label 'i' starting from the outer diameter machine (where the first slice corresponds to i = 1, the second slice for i = 2, etc.), model depth $L_{s,}$ and a total number of slices N are given. Eq. (2) provides the calculation for the value of $L_{s,}$ and Eq. (3) is employed to determine the value of j [8]. The stack length L for the linear model can be obtained using Eq. (4).

Performing a 2D FEM analysis typically yields faster results than a 3D FEM analysis, albeit with a slight margin of error. This can be attributed to several factors. Firstly, the nonlinearity of the magnetic material introduces varying saturation rates at different radii [19]. Secondly, the errors arising from the conical structure of models produced for different radius values need to be fully accounted for. The sensitivity of the 2D model analysis is also influenced by factors such as slotless machines or

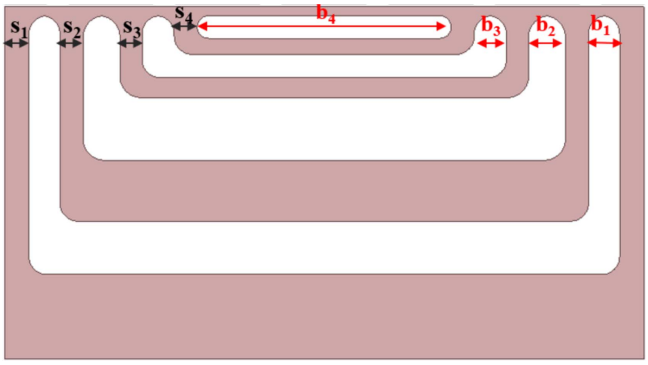

Fig. 4. (Color online) 2D Linear Model Representation of AF-SynRM Rotor Structure.

slot structures and the shape of the magnets they contain [10, 20]. Another parameter influencing the analysis sensitivity is the number of meshes employed. Due to its structural characteristics, the 2D linear model can be analyzed with fewer meshes than the 3D model. Fig. 3 illustrates the mesh structure of the 2D linear model.

Utilizing a conical structure in the AF-SynRM investigated in this study results in variations in the dimensions of barriers and tooth widths across different slices. Although there is proportionality in the dimensioning process, the conical structure causes differences between the individual slices compared to the results obtained from the 3D model analysis. The horizontal dimensions of the rotor segment and barrier in the AF-SynRM rotor are given in Fig. 4. These dimensions vary depending on the average diameter. The changes in the dimensions of rotor barriers and segments analyzed within the multislice model are provided in Table 2. It can be seen that the rotor dimensions, which have a conical structure, decrease to some extent from the outer diameter to the inner diameter.

This study of the 2D linear model for the AF-SynRM aimed to test the results by incorporating multiple slices. Multislice models were employed to achieve this,

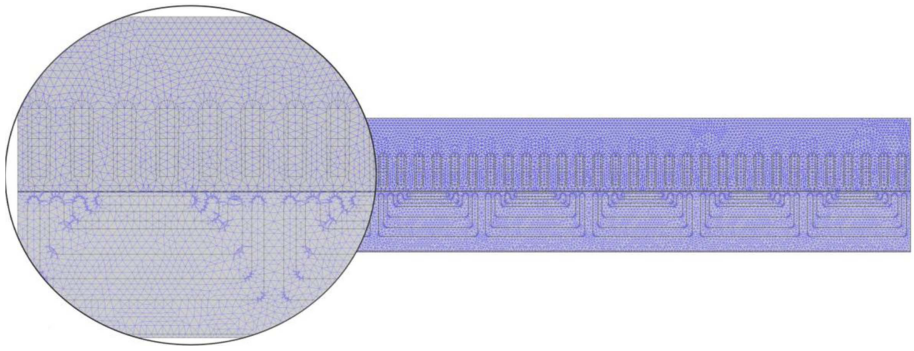

Fig. 3. (Color online) AF-SynRM Motor 2D Model Mesh Analysis.

Table 2. Change on rotor dimensions depending on average of diameter.

D_{avg} (mm)	Segments (mm)				Barriers (mm)			
	s_1	s_2	s_3	s_4	b_1	b_2	b_3	b_4
150	2.249	2.129	2.035	2.115	2.868	3.392	2.969	23.389
155	2.324	2.200	2.102	2.186	2.964	3.506	3.068	24.169
160	2.399	2.271	2.170	2.256	3.059	3.619	3.167	24.949
165	2.474	2.342	2.238	2.327	3.155	3.732	3.266	25.728
170	2.549	2.413	2.306	2.397	3.251	3.845	3.365	26.508
175	2.624	2.484	2.374	2.468	3.346	3.958	3.464	27.288
180	2.699	2.555	2.441	2.538	3.442	4.071	3.563	28.067
185	2.774	2.626	2.509	2.609	3.537	4.184	3.662	28.847
190	2.849	2.697	2.577	2.679	3.633	4.297	3.761	29.626
195	2.923	2.768	2.645	2.750	3.729	4.410	3.860	30.406
200	2.998	2.839	2.713	2.821	3.824	4.523	3.959	31.186
205	3.073	2.910	2.780	2.891	3.920	4.636	4.058	31.965
210	3.148	2.981	2.848	2.962	4.015	4.749	4.157	32.745

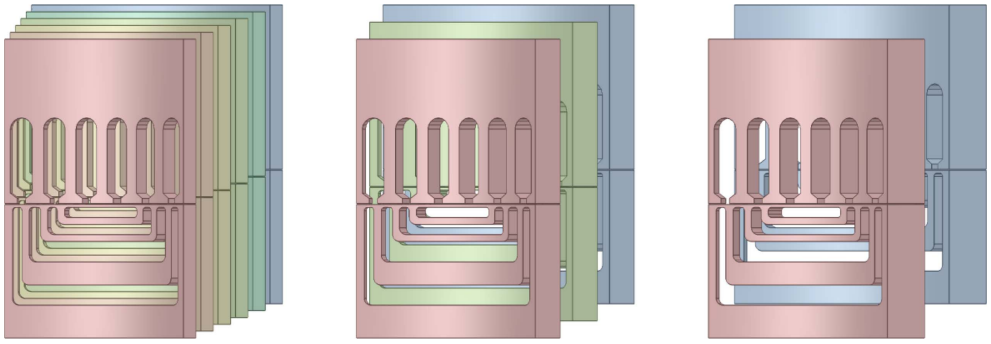

Fig. 5. (Color online) AF-SynRM Motor Multislice Models; 6 Slice, 3 Slice, 2 Slice.

dividing the model into different numbers of slices [21-23]. Initially, analyses were conducted using a single slice model. Subsequently, the number of slices was increased, and multislice models consisting of two, three, and six slices were created. These multislice models were generated using sequential and equivalent thickness slices, as illustrated in Fig. 5.

3. Analytical Results and Experiments Validation

The linear model design for AF-SynRM is based on some analytical calculations. The inductance values, L_{dm} and L_{qm}, for the d and q axes of the motor were determined through both FEM analyses and completed experimental tests. These inductance values were initially calculated using Eq. (5) for the linear model [24].

$$L_{dm} = \frac{B_{ad1}}{B_{a1}}.L_m = k_{dm1}.L_m$$
$$L_{qm} = \frac{B_{aq1}}{B_{a1}}.L_m = k_{qm1}.L_m \quad (5)$$

$$L_m = \frac{6\mu_0 (W_1 k_{w_1})^2 \tau L}{\pi^2 p.k_C.g_1(1+k_s)} \quad (6)$$

In the calculation of the magnetization inductance, B_{ad1}, and B_{aq1} represent the air gap flux density for d-q axes, B_{a1} denotes the uniform airgap, k_{dm1} and k_{qm1} are motor constants, and L_m signifies magnetization inductance. To determine the magnetization inductance, Eq. (6) is utilized, incorporating the following parameters: W_1 number of windings per phase, k_{w1} winding factor, τ pole pitch, p pole pair, g_1 mechanical gap, and k_s as the magnetic saturation factor are used [24].

$$F_{xpeak} = \frac{3}{2}\frac{\pi}{\tau}L_m\left(\frac{k_{dm1}}{1+k_{Sd}} - \frac{k_{dm1}}{k_{qm1}}\right)\left(I_{df_p}\sqrt{2}\right)\left(I_{qf_p}\sqrt{2}\right) \quad (7)$$

$$T_{xpeak} = F_{xpeak}.\frac{D_{avg}}{2} \quad (8)$$

Eq. (7) provides the peak value of the generated force F_{xpeak}. In this equation, I_{dfp} and I_{qfp} represent the current peak values of the d-q axes. However, for the 2D linear model, the torque result cannot be obtained due to the linear motion involved. To calculate the torque peak value T_{xpeak}, Eq. (8) is used, which involves force and average radius [24].

$$T_{ripple} = \frac{T_{\max} - T_{\min}}{T_{avg}} \quad (9)$$

Eq. (9) is used to calculate the torque ripple, which is determined by considering the maximum torque T_{max}, minimum torque T_{min} and average torque T_{avg} [24].

$$P_m = F_x U = \frac{3}{4}\frac{V_s^2(\omega_r L_d - \omega_r L_q)}{(R_s^2 + \omega_r^2 L_d L_q)^2}[(\omega_r^2 L_d L_q - R_s^2)\sin 2\delta_v + R_s(\omega_r L_d + \omega_r L_q).\cos\delta_v - R_s(\omega_r L_d - \omega_r L_q)],$$
$$\omega_r = \frac{2v}{D_{avg}} \quad (10)$$

Eq. (10) provides the formula to calculate the generated electromagnetic power P_m for the 2D linear motor model. This equation incorporates various parameters: V_s represents the rms value of voltage, v denotes the linear velocity, ω_r represents the angular velocity, R_s signifies the resistance per phase, and δ_y represents the voltage angle between the d-q axes [24].

$$P_{loss} = P_{iron} + P_{mec} + P_{cu} \quad (11)$$

$$\eta = \frac{P_m}{P_m + P_{loss}} \quad (12)$$

In the design of the AF-SynRM linear model, the total loss P_{loss} is determined by summing the iron losses P_{iron}, mechanical losses P_{mec} and copper losses P_{cu} according to Eq. (11). The efficiency η is then calculated based on the output power P_m and the input power (sum of the output power and total losses) using Eq. (12) [4].

For AF-SynRM 1/8 3D solid model, various FEM analyses were conducted, including 3D and 2D (single slice, two slices, three slices, and six slices, as shown in Fig. 5) linear model simulations. The mesh number plays a crucial role in analyzing these models, as it directly affects the accuracy of the results. Increasing the mesh number leads to results closer to the actual values and proportionally increases the analysis time [25]. Consequently, minimizing this time becomes a significant consideration for designers. In this study, Table 3 presents the number of meshes and the corresponding analysis times obtained from the 3D FEM model and the 2D FEM model.

Table 3. Number of mesh and analyses time.

Analysis Model	Number of Mesh	Analysis Period (minute)
3D FEM	146516	85.15
2D FEM (Single Slice)	19365	5.45
2D FEM (Average of 2 Slice)	19801	5.81
2D FEM (Average of 3 Slice)	19669	5.71
2D FEM (Average of 6 Slice)	19552	5.65

The accuracy of the applied method was evaluated by performing 3D and 2D FEM analyses at a single speed (nominal speed) under various load conditions. Measurements were taken for torque, torque ripple, back-EMF, and L_d-L_q values under different shaft load conditions (25 %, 50%, 75 %, 100 %, and 115 %) to assess the method's accuracy. The corresponding graphs depicting these values are presented in Fig. 6.

In 2D multislice linear models, the analysis results of individual slices are evaluated separately to obtain the overall model result. The results for each slice are summed, and the total model value is determined according to Eq. (13) for torque, back-EMF, and L_d-L_q. Meanwhile, the average value is obtained for the torque ripple using the formula provided in Eq. (14).

$$T_{total} = \sum_{x=1}^{N} T_x$$
$$e_{total} = \sum_{x=1}^{N} e_x \quad (13)$$
$$(L_d - L_q)_{total} = \sum_{x=1}^{N}(L_{d_x} - L_{q_x})$$

$$T_{ripple_{total}} = \frac{\sum_{x=1}^{N} T_{ripple_x}}{N} \quad (14)$$

The torque values obtained from each slice for both the 2D linear and 3D models are presented in Fig. 6(a). Upon analyzing the torque values, it was observed that the single slice 2D FEM analysis yielded the closest result to the full load, with an error of 0.4 %. As the load level decreased, the deviation between the 3D and 2D models

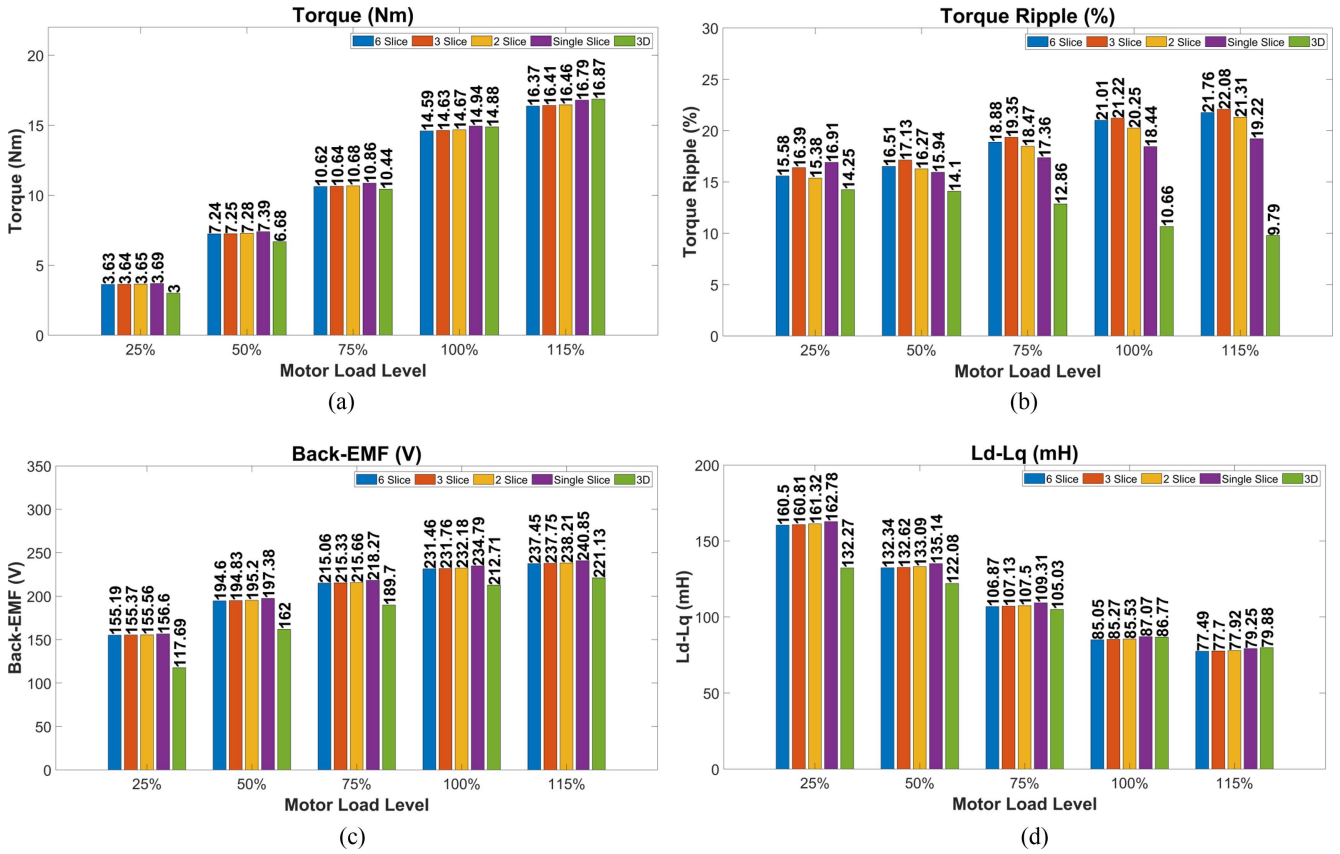

Fig. 6. (Color online) AF-SynRM Motor 3D, 2D Linear Model of Multislice Method; (a) Torque Analyses, (b) Torque Ripple Analyses, (c) Back-EMF Analyses, (d) L_d-L_q Analyses.

increased, although the results of the 2D model remained consistent. However, as depicted in Fig. 6(b), the torque ripple did not produce satisfactory results. The findings at full load indicated that the 2D single slice model exhibited the closest result among the multislice models. However, there was an approximately 72 % increase compared to the results obtained from the 3D model. This discrepancy can be attributed to the variation in slot and barrier dimensions caused by the conical structure of the axial flux machine, thus affecting the torque ripple values in the 2D model [5]. Another contributing factor to these differences is the negative impact of error components from harmonics in parameters such as back-EMF and current on the main constituent [10, 26]. While torque ripple increased for the 3D model, it decreased for the 2D linear model as the applied load on the motor shaft decreased. As shown in Fig. 6(b), the ripple values obtained under 25 % load were closely aligned. For the 3D model and the 2-slice multislice model, the margin of error was reduced to 8 %. Additionally, the results of the L_d-L_q analyses, as depicted in Fig. 6(c) and Fig. 6(d), were evaluated for model comparison. At full load, the back-EMF exhibited an error of approximately 10 % compared to the 3D model. Similarly, for L_d-L_q at full load, the error compared to the 3D model was about 1.8 %.

During the analyses, it was observed that increasing the number of slices did not provide a significant advantage

Fig. 7. (Color online) Test Bench.

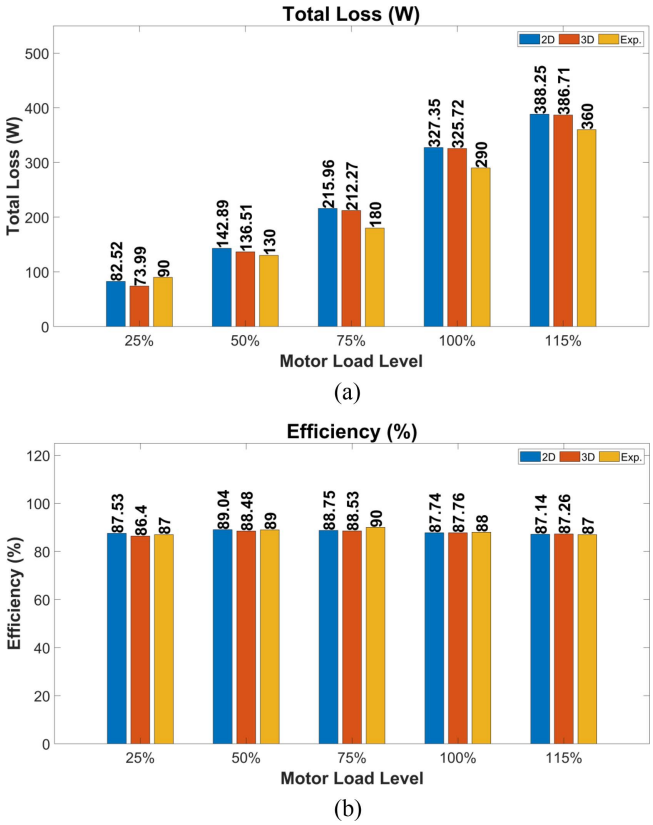

Fig. 8. (Color online) AF-SynRM Motor 3D, 2D Linear Model and Experimental Tests; (a) Losses Analyses, (b) Efficiency Analyses.

for the designer. The results obtained from the single slice model, created based on the average diameter, were very close to the 3D model. This is the most suitable solution, considering the reduction in analysis time. To validate the accuracy of this approach, experimental tests were conducted using the test setup illustrated in Fig. 7.

In Fig. 7, a 10-kW square body DC motor (labeled as '4') with a maximum speed of 4000 rpm and a nominal rate of 2270 rpm was employed to load the AF-SynRM (marked as '1'). The system torque measurements were conducted using load cell '6', while the speed was measured using encoder '7'. The control of the AF-SynRM was achieved with ABB ACS-880, while ABB DCS-550 was utilized for load-side control. A National Instrument Company NI cDAQ-9174 cabinet and NI9234-NI9225-NI9239 modules were employed to record the motor data. Under various shaft load levels (25 %, 50 %, 75 %, 100 %, 115 %), current, voltage, torque, and speed values were recorded at 1500 rpm [27].

After the evaluation, a comparison was made between the 3D and 2D linear models (Single Slice) and experimental results for various analyses. The losses and efficiency of the machine are presented in Fig. 8. It can be observed that the experimental results and results obtained from the 3D and 2D models closely resemble each other.

The 2D linear model exhibits an approximate 5 % margin of error compared to the 3D model for the total loss results at full load. The deviation between the 2D and 3D models increases as the load level decreases. The experimental results indicate that the values obtained are approximately 11 % lower than those predicted by the FEM analysis. The efficiency calculations yielded a minimal deviation of 0.02 % between the 2D and 3D model results. It is noteworthy that the experimental results align closely with these findings.

The total losses and efficiency of the motor were determined by averaging the results obtained from the 2D Linear multislice model analysis. It was observed that the slice results exhibited variability due to the different diameters. Consequently, increasing the number of slices would lead to additional analysis time without significant benefits. Therefore, utilizing a single slice 2D linear model appears advantageous due to its close agreement with the overall results.

4. Conclusion

Axial flux motors inherently possess a 3D flux model, which makes it challenging to perform 2D FEM as typically done for radial flux motors. Conducting a complete 3D analysis can be time-consuming, necessitating the use of various techniques to reduce computational time. In this study, a 2D linear model simulation was employed to approximate the behavior of the 3D AF-SynRM. Additionally, instead of employing 3D multislice solutions through 3D FEM analysis, the feasibility of using 2D linear models was tested.

The study initially examined the impact of the number of slices on the 2D FEM analysis of the AF-SynRM. The findings revealed that the single slice structure yielded results that closely aligned with the 3D analysis outcomes during the conversion from 3D to 2D. Increasing the number of 2D slices generally did not yield significant improvements in the FEM results. Consequently, it was demonstrated that a single slice structure is sufficient for the 2D model. In terms of computational efficiency, the 3D model (1/8 Solid model) required approximately 15 times more analysis time compared to the 2D linear model.

The subsequent part of the study involved comparing the results obtained from the single slice 2D linear FEM, 3D FEM, and experimental tests. The comparison revealed

a difference of 0.3 % in the total losses between the 2D linear model and 3D model analyses. Furthermore, the efficiency results indicated a negligible error of 0.02 % between the 3D and 2D linear models.

The results obtained from the analysis indicate that the 3D FEM analysis took approximately 85.15 minutes to complete, whereas the 2D linear FEM analysis was completed in about 5.45 minutes. Considering the close similarity in results between the two methods and the significant time savings offered by the 2D linear model, it is highly advantageous for designers. Its ability to provide accurate results with a minimal margin of error and reduced analysis time makes it a valuable tool in the design process.

Based on the obtained results, utilizing the 2D linear model for optimization in motor design can significantly save designer's valuable time. Exploring how the 2D linear model affects optimization results can be an important direction for future studies. Additionally, the multislice method can be employed to assess the impact and significance of the results obtained from each individual slice on the overall performance of the full model. This approach can provide further insights into the behavior of the motor and aid in making informed design decisions.

Acknowledgements

This study was supported by Tokat Gaziosmanpaşa University Scientific Research Projects Unit, project number 2020/41.

References

[1] A. Mahmoudi, S. Kahourzade, E. Roshandel, and W. L. Soong, in 2020 IEEE International Conference on Power Electronics, Drives and Energy Systems (PEDES), Jaipur, India: IEEE 1 (2020).
[2] G. Rodrigues Bruzinga, A. J. S. Filho, and A. Pelizari, IEEE Latin Am. Trans. **20**, 855 (2022).
[3] M. Özsoy, O. Kaplan, and M. Akar, Electr. Eng. **104**, 4289 (2022).
[4] M. Akar, M. Eker, M. Özsoy, and H. S. Gerçekçioğlu, Machines **10**, 838 (2022).
[5] M. Gulec and M. Aydin, IET Electric Power Applications **12**, 195 (2018).
[6] K.-H. Kim and D.-K. Woo, IEEE Access **10**, 98842 (2022).
[7] C. Corey, J. H. Kim, and B. Sarlioglu, in 2019 IEEE Energy Conversion Congress and Exposition (ECCE), Baltimore, MD, USA: IEEE 2996 (2019).
[8] A. Parviainen, M. Niemela, and J. Pyrhonen, IEEE Trans. on Ind. Applicat. **40**, 1333 (2004).
[9] A. Nyitrai, G. Szabó, and S. R. Horváth, Period. Polytech. Elec. Eng. Comp. Sci. **66**, 205 (2022).
[10] A. Egea, G. Almandoz, J. Poza, and A. Gonzalez, in The XIX International Conference on Electrical Machines - ICEM 2010, Rome, Italy: IEEE 1 (2010).
[11] B. Dianati, S. Kahourzade, and A. Mahmoudi, IEEE Trans. Energy Convers. **35**, 1522 (2020).
[12] A. Nobahari, A. Darabi, and A. Hassannia, in 2017 8th Power Electronics, Drive Systems & Technologies Conference (PEDSTC), Mashhad, Iran: IEEE 353 (2017).
[13] H. S. Gercekcioglu and M. Akar, Int. Trans. Electr. Energ. Syst. **31**, (2021).
[14] Q. Wei, F. Yu, Z. Xi, and L. Shuo, in 2011 International Conference on Electrical Machines and Systems, Beijing, China: IEEE, Aug. 1 (2011).
[15] B. P. B. Arthur and U. Baskaran, Sādhanā **45**, 134 (2020).
[16] M. Stepien, J. Mikos, A. Kallaste, and A. Rassolkin, in 2019 20th International Symposium on Power Electronics (Ee), Novi Sad, Serbia: IEEE 1 (2019).
[17] J. S. Kim, J. H. Lee, J.-Y. Song, D.-W. Kim, Y.-J. Kim, and S.-Y. Jung, IEEE Trans. Magn. **53**, 1 (2017).
[18] H. Tiegna, A. Bellara, Y. Amara, and G. Barakat, IEEE Trans. Magn. **48**, 1212 (2012).
[19] T. Wolnik (2020).
[20] H. Tiegna, Y. Amara, and G. Barakat, IEEE Trans. Magn. **50**, 817 (2014).
[21] C. Hong, W. Huang, and Z. Hu, IEEE Trans. Magn. **55**, 1 (2019).
[22] M. Dhifli, H. Ennassiri, Y. Amara, and G. Barakat, in 2016 XXII International Conference on Electrical Machines (ICEM), Lausanne, Switzerland: IEEE 2431 (2016).
[23] B. P. B. Arthur and U. Bhaskaran, J. Inst. Eng. India Ser. B **100**, 41 (2019).
[24] I. Boldea, Linear Electric Machines, Drives, and MAGLEVs Handbook, 1st ed. CRC Press (2017).
[25] M. Eker and M. Özsoy, Academic Platform Journal of Engineering and Smart Systems **10**, 94 (2022).
[26] A. Abdelli, A. Gilson, B. Chareyron, and G. Zito, in 2023 IEEE Workshop on Electrical Machines Design, Control and Diagnosis (WEMDCD), 1 (2023).
[27] M. Eker, Ph.D., Tokat Gaziosmanpaşa University, Department of Mechatronics Engineering (2018).